Journal of Rehabilitation in Civil Engineering 8-1 (2020) 50-62

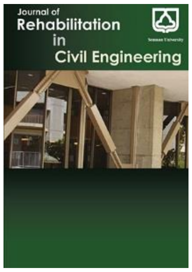

journal homepage: http://civiljournal.semnan.ac.ir/

A New Method for Calculating Earthquake Characteristics and Nonlinear Spectra Using Wavelet Theory

A. Heidari[1*], J. Raeisi[1], Sh. Pahlavan Sadegh[1]
1. Department of Civil Engineering, Shahrekord University, Shahrekord, Iran.

Corresponding author: *heidari@eng.sku.ac.ir*

ARTICLE INFO

Article history:
Received: 30 June 2018
Accepted: 10 October 2019

Keywords:
Strong Ground Parameters,
Nonlinear Spectrum Response,
Wavelet Theory,
Wavelet Denoising.

ABSTRACT

In the present study applying the wavelet theory (WT) and later the nonlinear spectrum response of the acceleration (NSRA) resulted in estimating a strong earthquake record for the structure to a degree of freedom. WT was applied in order to estimate the acceleration of earthquake mapping with equal sampling method (WTESM). Therefore, at first, the acceleration recorded in an earthquake using WTESM was examined in 5 levels. Subsequently, for calculating the strong ground parameters (SGP) and the NSRA of the structure the filtered wave was applied rather than using the main earthquake record (MER). The wavelet stages result in a more lenient filtered wave and it is better for calculating SGP and NSR because the noise is filtered. The method suggested for a large number of earthquakes was applied and the results are detailed in the case of Kermanshah earthquake. Results revealthat in case of using WTESM, SGP error estimation would be less than 2% and the calculation error for NSRA would be less than 11%.

1. Introduction

In earthquake engineering, the three main characteristics of the earth's motion are amplitude, frequency, and time (duration), and they are of great importance. As such, various parameters have been proposed with the aim of determining the characteristics of the strong ground parameters (SGP); some of these parameters are just one of the characteristics described earlier [1,2]. Domain parameters commonly applied in seismic analysis are the maximum acceleration and speed of the earth obtained by analyzing time histories, which is the major tool for performance-based seismic designs. Frequency content parameters describe the distribution of the range of motion of the earth at various frequencies. Since the frequency of earthquake movements is strongly affected by these movements, it is impossible to determine the

DOI: 10.22075/JRCE.2019.15255.1284

characteristics of the movement, by not deliberating its frequency.

Various parameters have been introduced for contemplating the frequency of earthquake. For instance, Rathje et al. provided models to predict the average earthquake periods for hard surface and rocky soils [3].

One of the methods that can be applied in order to isolate high earthquake frequencies is the wavelet transform. Wavelet transformation can be used to analyze the time-frequency of the earthquake wave to determine the time of occurrence of each frequency [4]. Wavelet transformation has also been used to optimize structures [5-9]. Moreover, the damage caused by earthquake buildings can be obtained through wavelet transform. Pnevmatikos and Hatzigeorgiou applied a discrete wavelet transform to examine the impact of the frame under the impact of the earthquake and the numerical results of this study revealed the positive effect of WT on the failure of the frame. In another study, an effective method was proposed for structural vulnerability. Through this method, it became possible to detect sudden changes in the vibration response by analyzing the transient response or velocity using the discrete wavelet transform. This examination was also done by applying the discrete wavelet transform of the earthquake [10]. Heidari and Raeisi proposed a new method to optimum design of structures for seismic loading by simulated aanealing using WT. the result reveals discrete wavelete transform and reverse wavelet transform were an effective approach for reducing the computational cost of optimization [11].

The study of the characteristics of the response spectrum of the structure is suitable for the recognition of the performance of structures with different erosion against earthquakes [12,13]. In the present study, in addition to the parameters of the SGP, the NSR of accelerated structure with single degree of freedom (SDOF) ductility is drawn. The NSRA of a SDOF structure has also been performed for the 5 stages of WTESM.

The earthquake wave is filtered in 5 stages applying WT and mother wavelet db4 stages in the present study. In order to achieve this, a WTESM was used. Throughout method, the number of accelerated earthquake record is not reduced and only high wave frequencies are eliminated at each stage and a new wave of lower and softer frequencies were obtained. Since the curve has become softer at each stage of the decomposition, the calculation time is somewhat reduced and an acceptable error is obtained. At each stage of wavelet decomposition, half of the noise (high frequencies) of the previous wave was eliminated. The main wave of the earthquake is decomposed with the transformation of the wavelet and its high and low frequencies are divided into two waves, which include details and approximate waves. Approximate wave is applied as a new earthquake wave, because previous research has demonstrated that it has the greatest effect on the dynamic response of the structure and it is highly similar to the main wave of the earthquake [6]. In the next step, the approximate wave was regenerated into two new waves, which include approximations and details. Moreover, the wave of approximations obtained at this stage is contemplated as a new wave and a wave of approximations and new details are obtained. This study was carried out in 5 steps. This method is known as discrete wavelet decomposition and was used to compute a number of SGP that yielded acceptable results [14].

After wave decomposition with wavelet theory in 5 consecutive stages and having 5 different approximation waves, NSR and SGP were obtained for each of the five stages. As a result of this, firstly, the NSR and main earthquake parameters (A) were calculated using the main accelerometer of the earthquake. Subsequently the parameters NSR and SGP for the approximate wave (A1) obtained in the first step were calculated. In the next step, NSR and SGP were obtained again for the wave approximation of the second stage (A2). This was performed for each of the 5 waveforms and then the difference in the values obtained for these 5 waveforms and the main wave of the earthquake was calculated.

Thirty earthquakes have been investigated through applying this method and the results for the Sarpolzahb earthquake record are presented in this article [15,18]. The results for the Kermanshah earthquake for Sarepolzahab record (SPZR) have shown that the decomposition error of the third wavelet is appropriate. The error rate for calculating the NSR of acceleration in the first two stages is about 1% and in the third, fourth and fifth stages, respectively, it is 11, 22, and 95%. Furthermore, the results revealed that the percentage of SGP by using wavelet method in the first two stages and in the third, fourth and fifth stages, is 1%.

2. Wavelet Theory

The wavelet transformation (WT) is applied to analyze the time series where the variance and mean value vary over time [19, 20]. Comparing WT with the Fourier transform is a attempt in order to gain better undertasnding. Fourier transforms a wave into different energies of the sinusoidal waves and frequency, without mentioning the frequency of occurrence. Localization is achieved on time by applying the FT in a window from time to time and moving it over a series of times, thus converting the FT, a Fourier window. However, the window length is taken to be constant regardless of the frequency. Unlike FTs, the WT adjusts the length of the analyzer window to go well with the frequency. By increasing the frequency accompanying the time series, the wavelet scale decreases and on the contrary, it increases with the frequency reduction of the wavelet scale. The WTs are divided into two types: continuous and discrete. The continuous mode advantage over the discrete is because of its ability to identify, extract, and analyze the total scales or frequencies of the time series. While the discrete transforms analyzes a limited number of scales [21]. The continuous wavelet transform (CWT) is similar to FT and is expressed as follows:

$$CWT_s^{\psi} = \frac{1}{\sqrt{|a|}} \int s(t)\psi^*_{a.b}(t)dt \qquad (1)$$

This Equation, is a function of two variables a and b. b is the transition, while a is the scale and it corresponds to the period (inverse frequency). Moreover, * symbolizes the conjugate conjugate. s is the main wave (in the present study it is the earthquake wave) and ψ is the mother wavelet functions. Mother's statement is applied because of the different functions used to convert the wavelet are all derived from the main function (mother). In other words, the mother wave is the main wave to produce other functions. All functions $\psi^*_{a,b}$ constructed from the maternal function are called wavelet functions or daughter functions and are derived from the following relationship:

$$\psi_{a.b}(t) = \psi(\frac{t-b}{a}) \qquad (2)$$

A discrete wavelet transform is a wavelet series that is sampled from continuous wavelet transform. In order to calculate the discrete wavelet coefficients, it is enough to replace the values of a and b in Equation 1 with $a=a_0^j$ and $b=ka_0^j b_o$.

$$\psi_{j.k}(t) = \frac{1}{\sqrt{a_0^j}}\psi(\frac{t-ka_0^j b_0}{a_0^j}) \tag{3}$$

After simplifying Equation 3, then we have:

$$\psi_{j.k}(t) = a_0^{\frac{-j}{2}}\psi(a_0^{-j}t - kb_0) \tag{4}$$

By dividing the discrete wavelet Equations, it is defined as follows:

$$DWT_s^{\psi} = \int_{-\infty}^{+\infty} s(t)\,\psi_{j.k}^*(t)dt \tag{5}$$

The applied method, namely sub-band coding on earthquake signals, has been applied in previous studies for signals in electrical engineering [22].

In this study, the stated method was used to analyze earthquake records for the first time where the main earthquake record is divided into two parts of high and low frequencies. Low and high frequencies of earthquake record are called approximate and detail, respectively. In DWT, low frequencies of earthquake record are used and the detailed part is ignored. Another sub-band coding is applied for the approximation part which is divided into two parts of approximate and detail.

Figure 1 portrays the decomposition of the earthquake record of Kermanshah in Sarpolzahab in Iran using WTESM. At the first level of the main earthquake record, two signals A1 and D1 were obtained, where A1 and D1 are the approximation and detail, respectively. The comparison between Figures 1.1 and 1.0 is that the A1 seen is similar to MER. Then in Figure 1.2, signal A2 is obtained from A1. The signal A2 is similar to A1. In Figure 1.3, signal A3 is obtained from A2. The signal A3 is similar to A2. This process continues for five levels.

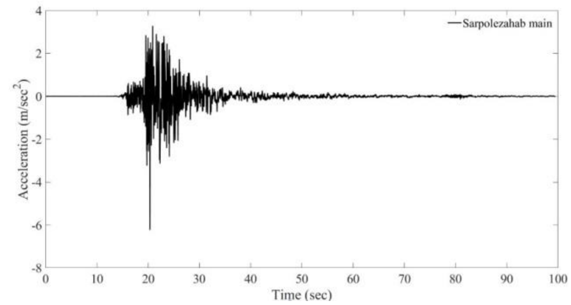

Fig. 1.0. Main earthquake record of Kermanshah in Sarpolzahab.

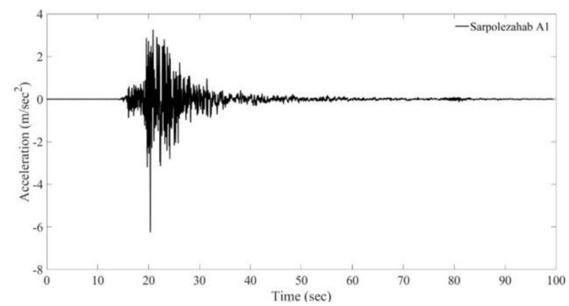

Fig. 1.1. WTESM of Sarpolzahab earthquake record in level 1 (A1).

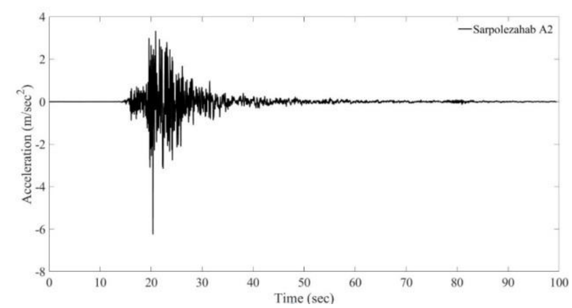

Fig. 1.2. WTESM of Sarpolzahab earthquake record in level 2 (A2).

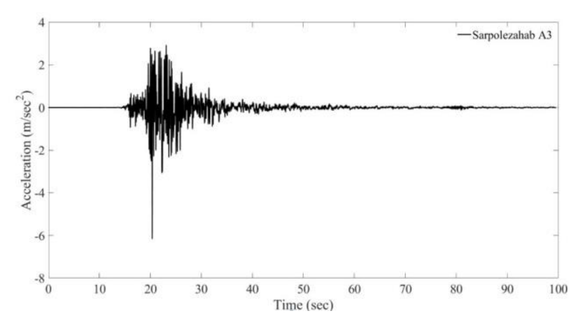

Fig. 1.3. WTESM of Sarpolzahab earthquake record in level 3 (A3).

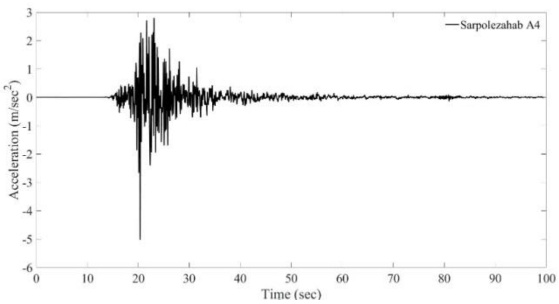

Fig. 1.4. WTESM of Sarpolzahab earthquake record in level 4 (A4).

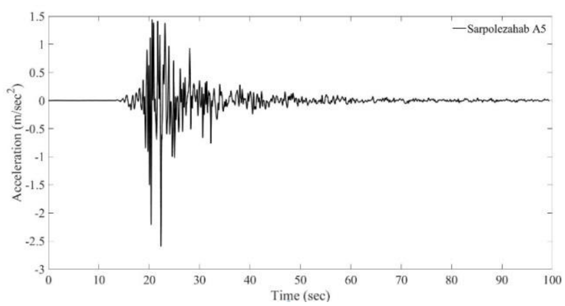

Fig. 1.5. WTESM of Sarpolzahab earthquake record in level 5 (A5).

3. Strong Ground Parameters (SGP)

Amplitude, frequency, and duration of motion are the three main characteristics of ground motion for earthquake engineering applications. Many parameters have been developed in order to determine these characteristics of SGP. Some of these parameters describe only one of the characteristics. Three main ground characteristics which include the amplitude, frequency content, and duration of movements are subsequently described briefly. Amplitude parameters, such as acceleration, velocity, or displacement or all of them can be determined using time history. Amplitude parameters describe only the peak amplitude for the unique cycle from the time history of ground motion. Frequency content parameters describe the distribution of ground motion amplitude in different frequencies. The frequency content of earthquake motions largely depends on these movements. Motion duration parameters have a major effect on the earthquake destructions. The duration of SGP depends on the time required to release cumulated strain energy along a fault.

Peak ground acceleration (PGA) is the maximum recorded acceleration value in an earthquake. The maximum value of the recorded characteristic in the velocity-time graph of an earthquake is called the peak ground velocity (PGV) and the maximum displacement in the ground surface obtained from the displacement-time graph is the peak ground displacement (PGD). The ratio between PGV and PGA is displayed along with PVA. The acceleration spectral intensity (ASI) is known as the spectral acceleration integral of SGP that its value is usually between 0.1 and 0.5 s and it is used to express the SGP magnitude. In addition, the velocity spectral intensity (VSI) is the spectral velocity integral of the SGP and it shows the SGP magnitude. The third or fifth large value of acceleration or velocity time history is the sustained maximum acceleration (SMA) and sustained maximum velocity (SMV) of the earthquake record and it shows the frequency content of SGP. The A95 parameter shows the maximum value of earthquake acceleration in relation to 95% of Arias intensity. The root-mean-square acceleration (a_{RMS}) shows the average intensity of earthquake acceleration and can be determined as follows:

$$a_{RMS} = \sqrt{\frac{1}{T_d}\int_0^{T_d}[s(t)]^2 dt} \tag{6}$$

where s(t) is the acceleration of ground motion and T_d is the duration of the SGP.

The root-mean-square velocity (V_{RMS}) shows the average intensity of the earthquake velocity and can be determined as follows:

$$V_{RMS} = \sqrt{\frac{1}{T_d}\int_0^{T_d}[v(t)]^2 dt} \quad (7)$$

where v(t) is the velocity-time ground motion.

The root-mean-square displacement (D_{RMS}) reveals the average intensity of earthquake displacement and can be determined as follows:

$$D_{RMS} = \sqrt{\frac{1}{T_d}\int_0^{T_d}[d(t)]^2 dt} \quad (8)$$

where d(t) is the displacement-time ground motion.

The Arias intensity (I_a) for every earthquake demonstrates the energy value taken by the structure which is expressed as follows [23]:

$$I_a = \frac{\pi}{2g}\int_0^{T_d}[s(t)]^2 dt \quad (9)$$

The characteristic intensity (I_C) has a linear relation with structural failure index, because of the maximum deformations and attracted hysteretic energy and is determined as follows [24]:

$$I_C = (a_{RMS})^{\frac{3}{2}}.\sqrt{T_d} \quad (10)$$

The specific energy density (S_E) displays the frequency content and amplitude parameter of the earthquake and is determined using:

$$S_E = \frac{\beta_S \rho_S}{4}\int v^2(t)\, d \quad (11)$$

where β_s and ρ_s are the shear wave velocity and soil density of the sampling site, respectively.

The cumulative absolute velocity (CAV) is the area under the absolute acceleration graph. CAV can be used to show structural failure potentiality [25].

$$\mathrm{CAV} = \int_0^{t_{max}} |s(t)|\, dt \quad (12)$$

where t_{max} is the total duration of the ground motion.

The Housner intensity (I_H) shows the input energy and is proportional with the square integral of ground acceleration. This index can be obtained as follows [26]:

$$I_H = \frac{1}{t_2 - t_1}\int_{t_1}^{t_2} s(t) dt \quad (13)$$

4. Nonlinear Spectrum Response of the Acceleration

This study discusses the NSRA, which are beneficial in studying the characteristics of the response spectrum and constructing a spectrum of design and related dynamics of structures to computational guidelines. Design reflection spectra, which are frequently used in building codes, can be obtained from the statistical analysis of the spectrum of responses to a set of earthquake records. One of the methods for analyzing structures against earthquakes is the use of the structure response spectrum with a degree of earthquake freedom. The non-elastic system will not fluctuate around the initial equilibrium state after submission. The surrender causes the system to find its way to the initial position of the lateral transition and after the system vibration has ended, it stays still in a new equilibrium state that is different from the initial equilibrium state, meaning, in the system of permanent deformation [13]. The governing equation for the elastoplastic system is as follows:

$$\ddot{u}(t) + 2\xi\omega_n\dot{u}(t) + \omega_n^2 u_y(t)\bar{f_s}(u,\dot{u}) = -\ddot{u}_g(t) \quad (14)$$

Equation 14 is the nonlinear dynamical equation of the structure under the ground acceleration $\ddot{u}_g(t)$. In the Equation, $\ddot{u}(t)$, $\dot{u}(t)$ and $u_y(t)$ are acceleration, velocity, and displacement of the structure during the earthquake, ω_n is the natural frequency, and ξ is the damping ratio of the structure. The value $\overline{f_s}(u, \dot{u})$ is also obtained from the following equation.

$$\overline{f_s}(u, \dot{u}) = \frac{f_s(u, \dot{u})}{f_y} \quad (15)$$

where f_y is the force at the point of surrender and f_s (u, u ̇) is the resistive force of the structure. The non-dimensional coefficient of μ is a non-dimensional parameter, which is based on the absolute magnitude of the deformation of the elastoplastic system due to the earthquake (u_m) to deformation (u_y), for systems that undergo deformations beyond the elastic limit (Chopra, 2001). This comes from the following:

$$\mu = \frac{u_m}{u_y} \quad (16)$$

5. Investigation of Earthquake in Sarpolzahab

On Sunday, November 17, 2017, at 21:48:16, a local earthquake with 7.3 magnitude of the Iranian-Iraqi border region shook strongly in the province of Kermanshah around the city of Sarpolzahab. Then, the parameters of the strong Sarpolezahab earthquake record and the nonlinear spectrum of its acceleration are expressed applying the wavelet theory.

5.1 Strong Earthquake Movement

Table 1 illustrates the parameters of the SGP for the main record of Sarpolzahab earthquake and for the waves obtained from wavelet decomposition from the first to fifth stages. As a result of this, these parameters are first obtained for the main wave of the earthquake and then calculated for each of the waves as exhibited in Figures 1.1 to 1.5.

Table 2 reveals the percentage of difference between the parameters of the SGP in Sarpolzahab earthquake and the waveguides obtained in 5 wavelet filtering steps. As shown, the difference in the first and second stages is less than 1%, in the third stage it is less than 2%, in the fourth stage, it is less than 7% and in the fifth stage, it is less than 21%. Based on the results of this research, it can be concluded that in order to calculate the parameters of the powerful land movement, the filtered wave was used in the fourth phase wavelet instead of using the main wave of the earthquake. Also, the fifth wavelet was used to calculate some parameters such as PGV, PGD, VRMS, DRMS, VSI, SMV, IH and SE with a 10% error limit.

Table 1. Parameters of the Sarpolzahab earthquake filtered in different wavelet stages.

Ground motion parameters	Characteristics of Kermanshah earthquake record					
	Main (A)	A1	A2	A3	A4	A5
PGA	6.24	6.25	6.25	6.16	5.02	2.59
PGV	0.35	0.35	0.35	0.35	0.38	0.32
PGD	0.24	0.24	0.24	0.24	0.24	0.24
PVA	0.057	0.056	0.056	0.057	0.075	0.12
a_{RMS}	0.38	0.38	0.38	0.37	0.32	0.21
v_{RMS}	0.055	0.055	0.055	0.055	0.055	0.054
D_{RMS}	0.055	0.055	0.055	0.055	0.055	0.055
ASI	3.91	3.91	3.90	3.86	3.53	2.31
VSI	1.42	1.42	1.42	1.41	1.38	1.30
SMA	3.23	3.20	3.16	3.02	2.71	1.50
SMV	0.33	0.33	0.33	0.32	0.33	0.30
I_H	1.40	1.40	1.40	1.40	1.39	1.36
S_E	0.30	0.30	0.30	0.30	0.30	0.29
A95	6.19	6.20	6.21	6.12	4.98	2.57
I_a	2.35	2.35	2.34	2.19	1.64	0.72
I_c	2.37	2.37	2.37	2.25	1.81	0.98
CAV	13.69	13.69	13.67	13.21	11.40	7.77

Table 2. Proportion of variations in the parameters of the SGP for different wavelet stages.

Ground motion parameters	(A-Ai)/A*100				
	A1	A2	A3	A4	A5
PGA	0.16	0.16	1.28	19.55	58.49
PGV	0	0	0	8.57	8.57
PGD	0	0	0	0	0
PVA	1.75	1.75	0	31.58	110.52
a_{RMS}	0	0	2.63	15.79	44.73
v_{RMS}	0	0	0	0	1.81
D_{RMS}	0	0	0	0	0
ASI	0	0.25	1.27	9.72	40.92
VSI	0	0	0.70	2.82	8.45
SMA	0.92	2.16	6.50	16.10	53.56
SMV	0	0	3.03	0	9.09
I_H	0	0	0	0.71	2.86
S_E	0	0	0	0	3.33
A95	0.16	0.32	1.13	19.55	58.48
I_a	0	0.42	6.81	30.21	69.36
I_c	0	0	5.06	23.63	58.65
CAV	0	0.14	3.51	16.73	43.24
Average	0.09	0.25	1.88	6.74	20.65

5.2 Nonlinear Response Spectrum of Acceleration

Since it is necessary to normalize various spectrum response diagrams using statistical methods in order to have a nonlinear response spectrum for high and heady structures and to have a final response spectrum according to statute, we have used an applicable and strong algorithm to transform earthquake wave to basic and fractional parts deliberating that the mentioned method would remove a number of data, then noises and errors were eliminated. This way we have reviewed normalized and accurate responses and at the same time maintained and reviewed all points of the spectrum. Therefore, it is expected to need less earthquakes for having required response spectrum.

Figures 2 to 7 show the NSRA of the Sarpolzahab earthquake record for a SDOF structure for attenuation of 5% and different ductility for the main earthquake filtered with wavelet in 5 stages. It should be noted that for calculating the NSRA, the main wave of the earthquake is in consonance with its maximum acceleration.

Figure 2 presents the NSRA of the Sarpolzahab earthquake record plotted for 1.5 ductility. By examining Figure 2, it can be concluded that by increasing wavelet stages, the error rate increases as compared to the original earthquake. The error rate in the first to fifth wavelets in this formability is less than 1, 3, 11, 22, and 96%.

Figure 3 presents the NSRA for 2 ductility. In this formability, the error rate in the first to fifth steps of the wavelet is less than 1, 3, 11, 22, and 95%, respectively.

Figure 4 shows the NSRA plotted for 2.5 ductility. By analyzing this figure, it can be concluded that by increasing the wavelet stages, the error rate increases as compared to the MER. The error rate in the first to fifth wavelets is 1, 3, 11, 22 and 95%, respectively.

Figure 5 manifests the NSRA for 3 ductility. In this formability, the percentage of error in the first to fifth wavelets is 1, 3, 11, 22, and 94%, respectively.

Figure 6 displays the NSRA plotted for the shape of 3.5 ductility. It is observed that by increasing the wavelet stages, the error rate increases with the MER. The error rate in the first to fifth wavelets in this formability is 1, 3, 11, 22, and 94%, respectively.

Figure 7 illustrates the nonlinear spectra of earthquake acceleration as shown in Figure 3.5. In this formability, the error rate in the first to fifth wavelets is 1, 3, 11, 22, and 94%, respectively.

The results of the investigation of the NSRA for attenuation of 5% and various deformations reveal that the error rate in the first to fifth wavelets is 1, 3, 11, 22, and 95%, respectively.

6. Conclusion

Using DWT, at every level, the low and high frequencies are separated. At the first level, the frequencies that are the largest and have had the lowest effect are eliminated and this is set as a rule. The high frequencies are eliminated for higher levels at each level though a number of accelerogram data would be out of hand this way. The results demonstrate that errors are not significant until the third level. In fact, up to level three, the high frequencies have been eliminated three times and hence the errors occur. These are the weak points for the wavelet theory. The strong ground motion parameters under study can help in selecting suitable earthquakes for dynamic analysis of structures. Therefore, the number of accelerogram is reduced by eliminating the largest frequencies in each level. This reduces the time required for for dynamic analysis especially for methods that are unconditionally stable like Linear Newmark method.

This research presents the results of the study of the strong earthquake movement parameters and the nonlinear response spectrum of the Kermanshah earthquake acceleration for the component registered in Sar-e-Pol-e Zahab. The results showed that:

The percentage difference between the parameters of the strong earthquake movement for the first earthquake and the first to fifth wavelets for all parameters in the first and second stages is less than 1%, in the third stage it is less than 2%, in the fourth stage it is less than 7%, and in the fifth stage, it is less than 21%.

- There is an error of about 10% for using the proposed method to calculate PGV, PGD, VRMS, DRMS, VSI, SMV, IH and SE parameters in the fifth step.
- For all the plasticity, the percentage difference of the non-linear acceleration response curve is less than 1, 3, 11, 22, and 95% in the first to fifth steps of the wavelet.

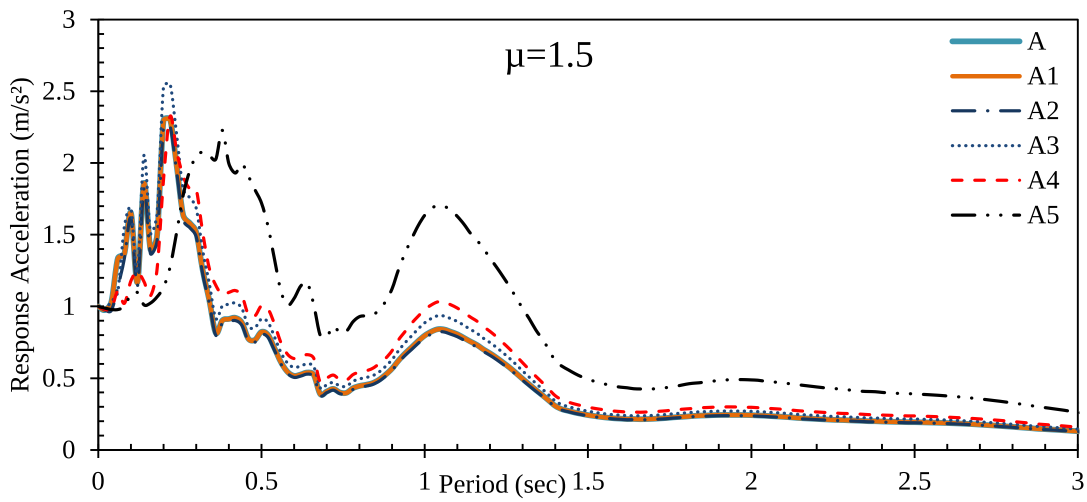

Fig. 2. NSRA of Sarpolzahab earthquake for 1.5 ductility for MER and various wavelet stages.

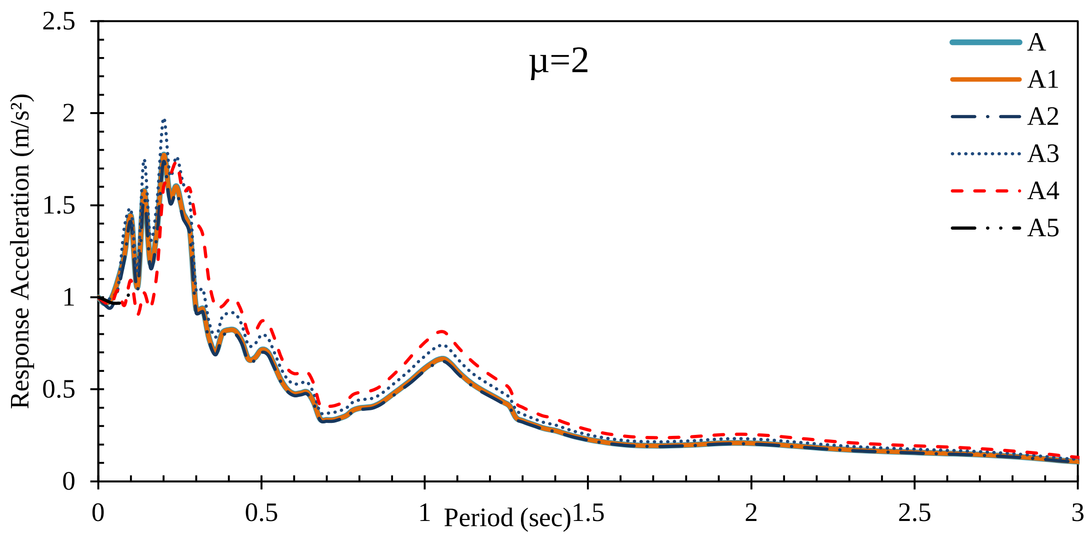

Fig. 3. NSRA of Sarpolzahab earthquake for 2 ductility for MER and various wavelet stages.

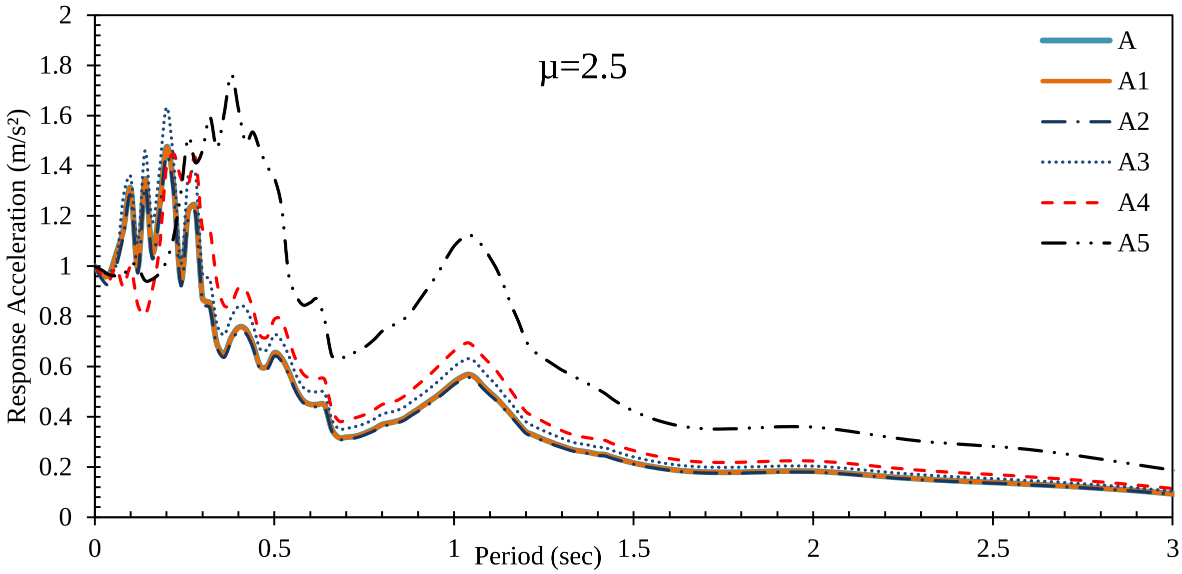

Fig. 4. NSRA of Sarpolzahab earthquake for 2 ductility for MER and various wavelet stages.

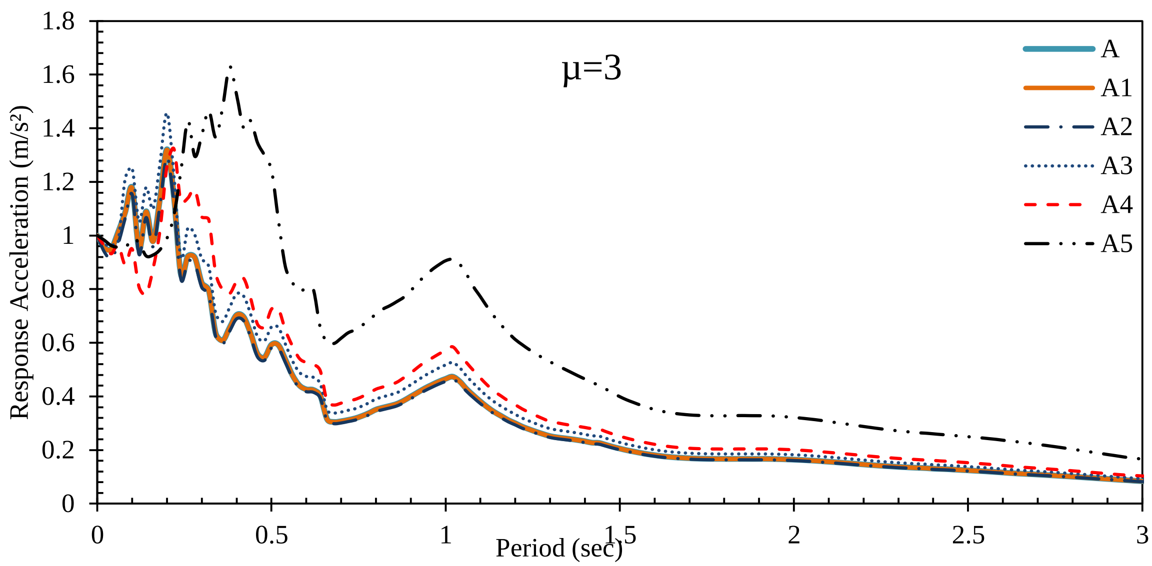

Fig. 5. NSRAof Sarpolzahab earthquake for 2 ductility for MER and various wavelet stages.

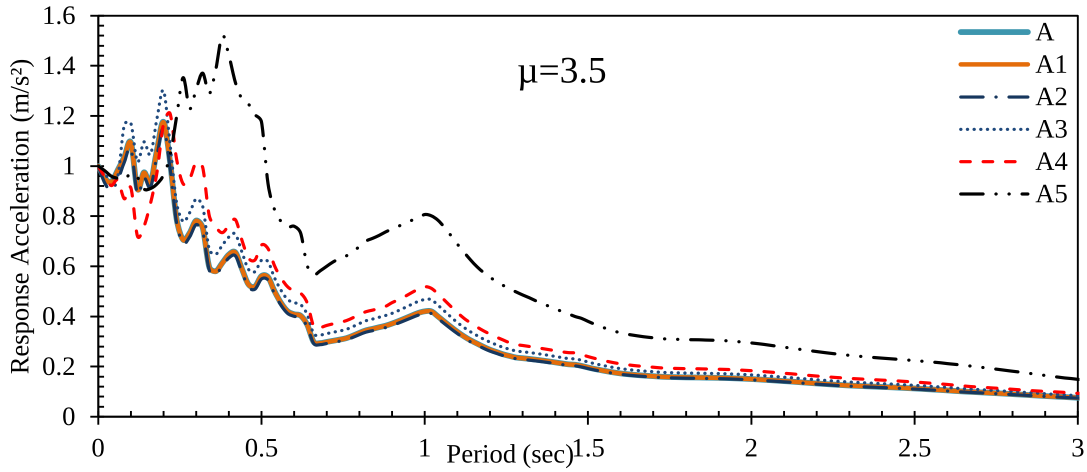

Fig. 6. NSRA of Sarpolzahab earthquake for 2 ductility for MER and various wavelet stages.

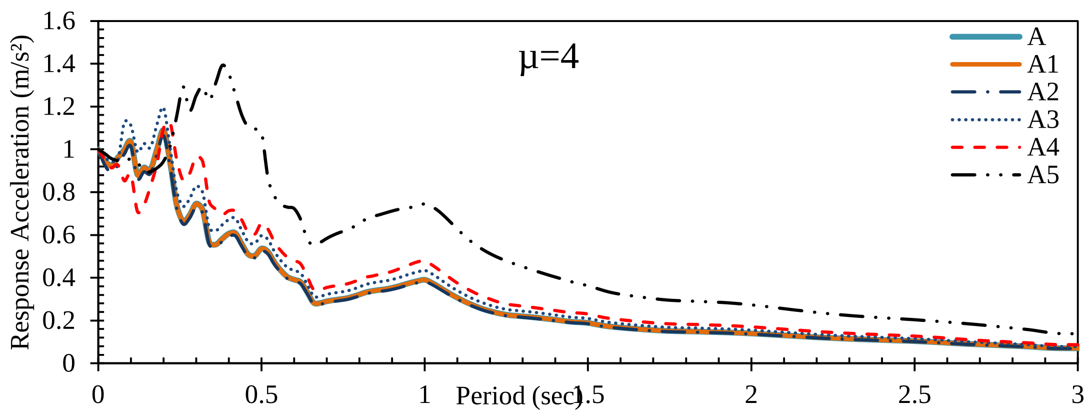

Fig. 7. NSRAof Sarpolzahab earthquake for 2 ductility for MER and various wavelet stages.

REFERENCES

[1] Boore, D. M. (1983). "Stochastic simulation of high-frequency ground motions based on seismological models of the radiated spectra." Bulletin of the Seismological Society of America, vol. 73, pp. 1865-1894.

[2] Yaghmaei-Sabegh, S., Ruiz-García, J. (2016). "Nonlinear response analysis of SDOF systems subjected to doublet earthquake ground motions: A case study on 2012 Varzaghan–Ahar" events. Engineering Structures, vol. 110, pp. 281-292.

[3] Rathje, E. M., Abrahamson, N. A., Bray, J. D. (1998). "Simplified frequency content estimates of earthquake ground motions. Journal of Geotechnical and Geoenvironmental Engineering." Vol. 124, pp. 150-159.

[4] Heidari, A., Salajegheh, E. (2008). "Wavelet analysis for processing of earthquake records." Asian Journal of Civil Engineering, 9(5), 513-524

[5] Salajegheh, E., Heidari, A. (2005a). "Optimum design of structures against earthquake by wavelet neural network and filter banks." Earthquake engineering & structural dynamics, vol. 34(1), pp. 67-82.

[6] Salajegheh, E., Heidari, A. (2005b). "Time history dynamic analysis of structures using filter banks and wavelet transforms." Computers & structures, vol. 83(1), pp. 53-68.

[7] Salajegheh, E., Gholizadeh, S., Torkzadeh, P. (2007). "Optimal desigin of structures with

frequency constraints using wavelet back propagation neural." Asian Journal of Civil Engineering, Vol. 8, pp. 97-111.

[8] Gholizadeh, S., Samavati, O. A. (2011). "Structural optimization by wavelet transforms and neural networks." Applied Mathematical Modelling, Vol. 35(2), pp. 915-929.

[9] Salajegheh, E., Gholizadeh, S. (2012). "Structural seismic optimization using metaheuristics and neural networks: a review." Computational Technology Reviews, Vol. 5(1), pp. 109-137.

[10] Pnevmatikos, N. G., Hatzigeorgiou, G. D. (2017). "Damage detection of framed structures subjected to earthquake excitation using discrete wavelet analysis" Bulletin of Earthquake Engineering, vol. 15, pp. 227-248.

[11] Heidari, A., Raeisi, J. (2018). "Optimum Design of Structures Against earthquake by Simulated Annealing Using Wavelet Transform." Soft Computing in Civil Engineering, doi: 10.22115/scce.2018.125682.1055

[12] Chopra, A.K. (1995). "Dynamics of Structures" vol. 3. Prentice Hall, New Jersey.

[13] Paz, M. (2012). "Structural dynamics: theory and computation." Springer Science & Business Media.

[14] Heidari, A., Raeisi, J., Kamgar, R. (2018). "APPLICATION OF WAVELET THEORY IN DETERMINING OF STRONG GROUND MOTION PARAMETERS." International Journal of Optimization in Civil Engineering, vol. , pp. 103-115.

[15] Raeisi, J. (2017). "Investigation of strong ground motion using a wavelet theory for hydraulic structure in far fault." MSc Thesis, Department of Civil Engineering, Shahrekord University, Iran. Shahrekord, Iran.

[16] Pahlavan-Sadegh, S. (2018). "Approximation of nonlinear m response spectrum of hydraulic structures using wavelet theory." MSc Thesis, Department of Civil Engineering, Shahrekord University, Shahrekord, Iran.

[17] Heidari, A., Raeisi, J., Kamgar., R., "The application of wavelet theory with denoising to estimate the parameters of earthquake". Scientia Iranica, Accepted Manuscript, 2019. DOI: 10.24200/SCI.2019.50675.1815

[18] Heidari, A., Pahlavan sadegh, S., Raeisi., J., "Investigating the effect of soil type on non-linear response spectrum using wavelet theory", International Journal of Civil Engineering, Accepted Manuscript, 2019, https://doi.org/10.1007/s40999-019-00394-6

[19] Daubechies, I. (1990). "The wavelet transform, time-frequency localization and signal analysis." IEEE transactions on information theory, vol. 36, pp. 961-1005.

[20] Naderpour, H., Fakharian, P., (2016), "A Synthesis of Peak Picking Method and Wavelet Packet Transform for Structural Modal Identification", KSCE Journal of Civil Engineering, Volume 20, Issue 7, pp 2859–2867; DOI: 10.1007/s12205-016-0523-4.

[21] Rioul O, Vetterli M. 1991. "Wavelets and signal processing." IEEE special magazine, pp. 14–38.

[22] Woods, J. W. (1991). "Subband image coding." Kluwer Academic Publishers, Dordrecht.

[23] Arias, A. (1970). "Measure of earthquake intensity", Massachusetts Inst. of Tech. Cambridge. Univ. of Chile, Santiago de Chile.

[24] Park, Y. J., Ang, A. H. S., Wen, Y. K. (1985). "Seismic damage analysis of reinforced concrete buildings." Journal of Structural Engineering, vol. 111, pp. 740-757.

[25] Kramer, S. L. (1996). "Geotechnical Earthquake Engineering." Prentice Hall. New York.

[26] Housner GW. (1975). "Measures of severity of earthquake ground shaking." In: Proceedings of the first US national conference on earthquake engineering, Ann Arbor, MI.